Output Feedback Formation Control of a School of Robotic Fish with Artificial Lateral Line Sensing

Artur Wolek and Derek A. Paley

Abstract— **This paper presents an estimation and control framework to stabilize the parallel motion of a school of robotic fish using sensory feedback. Each robot is modeled as a constant speed, planar, self-propelled particle that produces a flowfield according to a dipole potential flow model. An artificial lateral line system senses pressure fluctuations at several locations along each robot's body. The equations of motion and measurement model are formulated in a path frame that translates and rotates with each robot's position and velocity, respectively. A particle filter estimates the relative position and heading of other nearby robots. The resulting estimate drives a Lyapunov-based formation controller to synchronize the headings of the robots and achieve a parallel formation. Numerical simulations illustrate the proposed approach.**

I. Introduction

Bio-inspired underwater vehicles have been proposed as efficient, maneuverable, and stealthy mobile sensor platforms for numerous applications such as environmental monitoring, infrastructure inspection, surveillance, and subsea search. However, underwater vehicle coordination remains challenging due to limitations in underwater communication and sensing. Acoustic modems commonly used by conventional-propulsion underwater vehicles are too bulky and power-intensive to be used by small and simply instrumented bio-inspired designs. Instead, passive vision or hydrodynamic sensing can offer more compact sensing capabilities that mimic the sensory basis of real fish schools [1].

Hydrodynamic sensing is particularly useful in dark, murky, and cluttered environments where vision-based sensing is difficult. Many fish-inspired robots (referred to here as *fishbots*) have been developed to employ hydrodynamic sensing in the form of an artificial lateral line (ALL) system. An ALL system emulates the lateral line system of a real fish—an organ consisting of cell receptors called neuromasts that are distributed around the body and sense pressure gradients and flow velocities [2]. In an ALL system, the exterior of the fishbot is instrumented (commonly with pressure sensors) to extract information about the flow. Estimation and feedback control techniques based on ALL measurements have been demonstrated for a variety of single fishbot control objectives including speed control [3], rheotaxis or station holding [2], [4], wall following [5], trajectory tracking [6] [7], and Kármán gaiting [8]. ALL-based estimation and control techniques have also enabled leader-follower arrangements of two fishbots [9], [10], or identifying the center of mass and population of a three or more fishbots [11].

State estimation approaches that assimilate ALL measurements have been investigated using model-free and model-based techniques. Model-free methods use experimental or simulated training data and regression or neural networks to estimate robot states from time-series of pressure measurements [4], [9], [10], [12]. Model-based methods use an analytical flowfield representation with a parameter or dynamic state estimator (e.g., recursive Bayesian estimation [2], [3], [8]). Flow models based on potential flow theory have been proposed, including self-propelled dipole models [13], oscillating dipole models [9], [14], quasi-steady Joukowsky transformations [3], and discrete circulation shedding [7].

In this paper, an output feedback formation controller is developed to stabilize the parallel motion of a school of fishbots using ALL measurements. The fishbots are constant-speed self-propelled particles [15] that generate a flowfield based on a dipole potential flow model [13]. The dynamics and measurement equation are formulated in a path frame that translates and rotates with each fishbot, and a particle filter estimates the relative state of all agents. This approach supports the integration of control laws that require precise state feedback rather than those rely on aggregate or average statistics such as the center of mass [11].

The contributions of this paper are (1) a state-space model of the relative motion and spatially distributed pressure measurements for a school of robotic fish modeled as constant-speed self-propelled particles each generating a dipole flowfield; (2) a particle filter estimation framework to estimate the relative state of fishbots from onboard sensor measurements; and (3) an output-feedback control design that achieves parallel formations for the same system. The proposed estimation and control algorithms are illustrated through numerical simulations.

The remainder of the paper is organized as follows. Section II reviews self-propelled particle formation control and the dipole potential flow model. Section III develops the dynamics and measurements of the fishbot school in a path frame. Section IV presents the particle filter estimation framework. Section V describes the output-feedback control design for parallel formations and presents simulation results. Section VI summarizes the paper and suggests future work.

This work was partially supported by ONR Grant No. 115239289.

A. Wolek is an Assistant Professor with the Department of Mechanical Engineering and Engineering Science, University of North Carolina at Charlotte, Charlotte, NC 28223 USA (e-mail: awolek@charlotte.edu).

D. A. Paley is the Willis H. Young Jr. Professor of Aerospace Engineering Education in the Department of Aerospace Engineering and the Institute for Systems Research, University of Maryland, College Park, MD 20742 USA (e-mail: dpaley@umd.edu).

II. Preliminaries

This section reviews relevant background, including the self-propelled particle model, the corresponding parallel formation control law, and the dipole model of the flowfield produced by a collection of self-propelled particles.

A. Self-Propelled Particle Parallel Formations

The self-propelled particle model [15] has often been used to describe the collective motion of N planar vehicles that move at a constant speed with steering controls inputs. The planar position of the kth particle with respect to an inertial frame $\mathcal{I} = \{O, 1, i\}$ with origin O is expressed using complex coordinates as $r_k = x_k + iy_k \in \mathbb{C}$, where $k = 1, \ldots, N$. The dynamics of the kth particle are

$$\begin{aligned} \dot{r}_k &= v_k e^{i\theta_k} \\ \dot{\theta}_k &= u_k, \end{aligned} \tag{1}$$

where, for the kth particle, $v_k \triangleq \sqrt{\dot{x}_k^2 + \dot{y}_k^2} \in \mathbb{R}$ is a constant speed, $\theta_k \triangleq \operatorname{atan}(\dot{y}_k/\dot{x}_k) \in \mathbb{S}$ is the orientation of the velocity (also called the phase of the particle), and $u_k \in \mathbb{R}$ is the steering control. The unit vector $e^{i\theta_k}$ is called the phasor of particle k and is aligned with its direction of motion, whereas the phasor $ie^{i\theta_k}$ is rotated 90° in the counter-clockwise direction from $e^{i\theta_k}$.

When referring to the phase arrangement and control inputs of the collective of N particles, we use bold letters, i.e., $\boldsymbol{\theta} \triangleq [\theta_1, \ldots, \theta_N]^{\mathrm{T}} \in \mathbb{S}^N$ and $\boldsymbol{u} = [u_1, \ldots, u_N]^{\mathrm{T}} \in \mathbb{R}^N$, respectively. Similarly, $e^{i\boldsymbol{\theta}} \triangleq [e^{i\theta_1}, \ldots, e^{i\theta_N}]^{\mathrm{T}} \in \mathbb{C}^N$. For complex numbers, $z_1, z_2 \in \mathbb{C}$, the inner product is defined as $\langle z_1, z_2 \rangle = \mathrm{Re}\{\overline{z_1} z_2\}$, where $\overline{z_1}$ is the complex conjugate of z_1; this inner product is equivalent to the standard inner product on $\mathbb{R}^2$. For complex vectors, $\boldsymbol{z}, \boldsymbol{y} \in \mathbb{C}^N$, the inner product is similarly defined as $\langle \boldsymbol{z}, \boldsymbol{y} \rangle = \sum_{i=1}^N \mathrm{Re}\{\overline{z_i} y_i\}$. The modulus of a complex number is denoted $|\cdot| = \sqrt{\langle \cdot, \cdot \rangle}$.

Parallel formations can be achieved for the system (1) using Lyapunov-based control design to maximize a potential function for a desired formation. Consider the parallel formation potential [16]

$$U(\boldsymbol{\theta}) \triangleq \frac{N}{2}|p_\theta|^2 = \frac{N}{2}\langle e^{i\boldsymbol{\theta}}, e^{i\boldsymbol{\theta}} \rangle \ , \tag{2}$$

where the phase order parameter $p_\theta = \frac{1}{N}\sum_{k=1}^N e^{i\theta_k}$ measures the degree of synchrony in the formation. When $|p_\theta|$ reaches its maximum value of one the particles are synchronized ($\theta_j = \theta_k$ for all $j, k = 1, \ldots, N$). Under the gradient control [16]

$$u_k = -K\frac{\partial U}{\partial \theta_k} = -K\langle p_\theta, ie^{i\theta_k} \rangle = -\frac{K}{N}\sum_{j=1}^N \sin\theta_{jk} \ , \tag{3}$$

where $\theta_{kj} = \theta_k - \theta_j = -\theta_{jk}$, with $K < 0$, solutions of (1) converge to the synchronized state, unless they start in an unstable equilibrium condition [16].

B. Dipole Potential Flow Model

In a two-dimensional inviscid fluid, self-propelled bodies produce (to leading order) a dipolar velocity field modeled using potential flow theory [13]. The flow created by the particle (1) is generated by a pair of point vortices in a T-arrangement located to the left and right of the body [13] at positions

$$r_k^- = r_k + \frac{lie^{i\theta_k}}{2} \qquad \text{and} \qquad r_k^+ = r_k - \frac{lie^{i\theta_k}}{2} \ , \tag{4}$$

respectively, where l is the distance between the vortices, $r_k = (r_k^- + r_k^+)/2$ is the center point between the vortices, and θ_k is the orientation of the dipole. Assume the left vortex has positive circulation $\Gamma_k > 0$ and the right vortex has negative circulation $-\Gamma_k$. The conjugate velocity field resulting from N dipoles is [13]

$$w(z) = \sum_{k=1}^N \left(\frac{-i\Gamma_k}{2\pi}\right)\left(\frac{1}{z - r_k^-} - \frac{1}{z - r_k^+}\right) \ , \tag{5}$$

where the horizontal and vertical velocity components in frame $\mathcal{I}$ are $\mathrm{Re}\{w(z)\}$ and $-\mathrm{Im}\{w(z)\}$, respectively. Interaction of dipoles that influence each other's velocity has been studied in [13]. Here, we assume that the fishbots' dynamics are decoupled (i.e., each fishbot's speed is fixed) and the circulation strength is $\Gamma_k = 2\pi l v_k$.

III. Relative Motion and Measurement Model

This section re-formulates the self-propelled particle dynamics (1) and the dipole flow-model (5) in a path frame $\mathcal{B}_k = \{r_k, e^{i\theta_k}, ie^{i\theta_k}\}$ with origin at the kth fishbot's position r_k and orthonormal unit vectors $e^{i\theta_k}$ and $ie^{i\theta_k}$, which are aligned and perpendicular to the kth fishbot's velocity, respectively (see Fig. 1). Since fishbots can perceive hydrodynamic cues from nearby sources, the path frame is a natural choice for formulating the estimation problem. It also suitable for use with the parallel formation control law (3), which uses relative heading for feedback. By avoiding the need to track absolute positions, the path frame formulation lends itself to the underwater environment where navigation and perception are challenging.

A. Relative Motion Model

An arbitrary point $z = x + yi \in \mathbb{C}$ in the inertial frame $\mathcal{I}$ maps to a point $\tilde{z} = \tilde{x} + \tilde{y}i \in \mathbb{C}$ in the path frame $\mathcal{B}_k$ by

$$\tilde{z} = \Phi(z; r_k, \theta_k) = \langle z - r_k, e^{i\theta_k} \rangle + \langle z - r_k, ie^{i\theta_k} \rangle i \ , \tag{6}$$

where the $(\,\tilde{}\,)$ symbol is used to denote a point observed in $\mathcal{B}_k$. The mapping (6) projects the difference $z - r_k$ onto the basis of $\mathcal{B}_k$ such that $\mathrm{Re}\{\tilde{z}\}$ and $\mathrm{Im}\{\tilde{z}\}$ are the components along $e^{i\theta_k}$ and $ie^{i\theta_k}$, respectively. The inverse mapping is

$$z = \Phi^{-1}(\tilde{z}; r_k, \theta_k) = r_k + \tilde{x}e^{i\theta_k} + \tilde{y}ie^{i\theta_k} \ .$$

Using (6), the position of the jth fishbot observed from $\mathcal{B}_k$ is $\tilde{r}_{jk} = \Phi(r_j; r_k, \theta_k)$ and the position of the kth fishbot observed from j is $\tilde{r}_{kj} = -\tilde{r}_{jk} = a_{jk} + b_{jk}i$, where the forward and cross-track coordinates are

$$a_{kj} = \langle r_k - r_j, e^{i\theta_k} \rangle \quad \text{and} \quad b_{kj} = \langle r_k - r_j, ie^{i\theta_k} \rangle \ , \tag{7}$$

respectively. The relative position dynamics of fishbot j with respect to fishbot k are obtained by differentiating (7) along

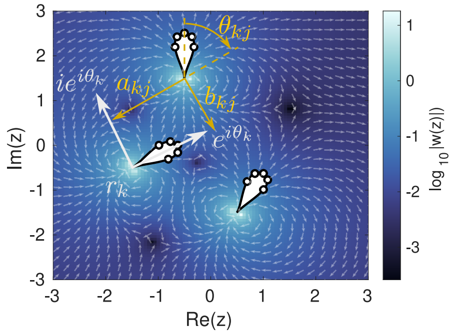

Fig. 1: Flow-field model with magnitude $|w(z)|$ in the complex plane induced by three dipoles. A hydrofoil shaped fishbot body is shown with circular markers to indicate the location of pressure sensors. The relative state of fishbot j with respect to fishbot k's path frame $B_k = \{r_k, e^{i\theta_k}, ie^{i\theta_k}\}$ is described by $(a_{kj}, b_{kj}, \theta_{kj})$.

trajectories of (1):

$$\begin{aligned} \dot{a}_{kj} &= v_k - v_j \cos\theta_{kj} + b_{kj} u_k \\ \dot{b}_{kj} &= v_j \sin\theta_{kj} - a_{kj} u_k \\ \dot{\theta}_{kj} &= u_k - u_j \ . \end{aligned} \tag{8}$$

Consider a homogeneous school of fishbots with equal speed, $v_k = v_j = v$ for all $j, k = 1, \ldots, N$ and identical circulation strength Γ. Estimation and control occurs periodically every $T = t_s - t_{s-1}$ seconds, where $s \in \mathbb{Z}$ is an integer index for the discrete time t_s. While (8) represents the actual dynamics of the system, for estimation purposes a simpler model is adopted wherein the kth fishbot assumes all of its neighbors have zero turn-rate, i.e., $u_j = 0$ for all $j \neq k$. Suppose that at time t_s the state of the system is given by a_{kj}, b_{kj}, θ_{kj} for all $j \neq k$. If the kth fishbot is turning with a constant input $u_k \neq 0$, then (8) is integrated from t_s to $t_{s+1} = t_s + T$ to give the new states:

$$\begin{aligned} a'_{kj} &= a_{kj}\cos(u_k T) + b_{kj}\sin(u_k T) + (v/u_k)\sin(u_k T) \\ &\quad + Tv\sin\theta_{kj}\sin(u_k T) - Tv\cos\theta_{kj}\cos(u_k T) \\ b'_{kj} &= -a_{kj}\sin(u_k T) + b_{kj}\cos(u_k T) \\ &\quad + (v/u_k)(\cos(u_k T) - 1) + Tv\sin\theta_{kj}\cos(u_k T) \\ &\quad + Tv\cos\theta_{kj}\sin(u_k T) \\ \theta'_{kj} &= \theta_{kj} + u_k T \ . \end{aligned} \tag{9}$$

If the fishbot is not turning, i.e., $u_k = 0$, the integration is

$$\begin{aligned} a'_{kj} &= a_{kj} + vT(1 - \cos\theta_{kj}) \\ b'_{kj} &= b_{kj} + vT\sin\theta_{kj} \\ \theta'_{kj} &= \theta_{kj} \ . \end{aligned} \tag{10}$$

B. Artificial Lateral Line Measurement Model

An artificial lateral line system (ALLS) assimilates measurements from N_p pressure ports on the perimeter of the kth fishbot located at positions $z_q \in \mathbb{C}$, $q = 1, \ldots, N_p$ in frame $\mathcal{I}$. Assuming a quasi-steady flow and applying Bernoulli's principle, the pressure measured at the qth sensor is [3]

$$p_q = p(z_q) - \frac{1}{2}\rho|w(z_q)|^2 \ , \tag{11}$$

where the first term $p(z_q)$ is the ambient pressure, the second term is the dynamic pressure, ρ is the fluid density, and $|w(z_q)|$ is the speed of the flow at sensor position z_q from (5). Under the assumption of quasi-steady flow, the pressure difference between sensors $q, r \in \{1, \ldots, N_p\}$ is [3]

$$\Delta p_{qr} = p_q - p_r = \frac{1}{2}\rho\left(|w(z_q)|^2 - |w(z_r)|^2\right) \ . \tag{12}$$

Equation (12) forms the basis of the fishbot's measurement model. To express (12) in terms of the relative coordinates (7), the left and right vortices of the jth fish (4) are mapped by (6) to frame $\mathcal{B}_k$:

$$\begin{aligned} \tilde{r}_j^- &= (-a_{kj} - (l/2)\sin\theta_{kj}) + (-b_{kj} + (l/2)\cos\theta_{kj})i \\ \tilde{r}_j^+ &= (-a_{kj} + (l/2)\sin\theta_{kj}) + (-b_{kj} - (l/2)\cos\theta_{kj})i \ . \end{aligned}$$

The kth fishbot's own vortices map to fixed locations in frame $\mathcal{B}_k$ with $\tilde{r}_k^- = -il/2$ and $\tilde{r}_k^+ = il/2$. The pressure sensor locations $\tilde{z}_q$ of the kth fishbot are also fixed in $\mathcal{B}_k$. Thus, the conjugate velocity at the qth pressure port of the kth fishbot is a sum of a variable term d_q (due to other fishbots) and a constant self-induced differential pressure c_q: $w(\tilde{z}_q) = d_q + c_q$, where

$$\begin{aligned} d_q &= \left(\frac{-i\Gamma}{2\pi}\right)\sum_{j\neq k}\left(\frac{1}{\tilde{z}_q - \tilde{r}_j^-} - \frac{1}{\tilde{z}_q - \tilde{r}_j^+}\right) \\ c_q &= \left(\frac{-i\Gamma}{2\pi}\right)\left(\frac{1}{\tilde{z}_q + il/2} - \frac{1}{\tilde{z}_q - il/2}\right) \ . \end{aligned} \tag{13}$$

The ambient pressure is constant across all sensors and the pressure differential (12) across two sensors $q, r \in \{1, \ldots, N_p\}$ with (12) is

$$\begin{aligned} \Delta p_{qr} = \frac{1}{2}\rho\,\big[&(|d_q|^2 + 2\langle d_q, c_q\rangle + |c_q|^2) \\ &- (|d_r|^2 + 2\langle d_r, c_r\rangle + |c_r|^2)\big] \ . \end{aligned} \tag{14}$$

The total combinatorial number of sensor pairs (excluding $q = r$) is $N_m = (N_p)!/2!/(N_p - 2)!$ [3].

Let the state of the jth fishbot relative to fishbot k be denoted by $[a_{kj}\ b_{kj}\ \theta_{kj}] \in \mathcal{X}$, where $\mathcal{X} = \mathbb{R}^2 \times \mathbb{S}$ and let $\boldsymbol{X} \in \mathcal{X}^{N-1}$ denote the state of all $N-1$ fishbots excluding the kth fishbot. The vector $\boldsymbol{X}$ is formed from $a_{kj}, b_{kj}, \theta_{kj}$ for all $j = 1, 2, \ldots, N$ with $j \neq k$ since $a_{kk} = b_{kk} = \theta_{kk} = 0$ is constant. The kth fishbot measures a $N_m \times 1$ vector of differential pressures from (14)

$$\boldsymbol{y} = \boldsymbol{h}(\boldsymbol{X}) + \boldsymbol{\eta} = \begin{bmatrix} \Delta p_{12,k}(\boldsymbol{X}) \\ \vdots \\ \Delta p_{(N_p-1)N_p,k}(\boldsymbol{X}) \end{bmatrix} + \boldsymbol{\eta} \ , \tag{15}$$

where $\boldsymbol{\eta} \sim \mathcal{N}(\boldsymbol{0}, \boldsymbol{\Sigma}_y)$ is uncorrelated zero-mean Gaussian sensor noise with covariance $\boldsymbol{\Sigma}_y = \boldsymbol{1}_{N_m \times N_m}\sigma_y^2$.

IV. Particle Filter Estimation

This section describes a particle filter that estimates the relative state of neighboring fishbots from artificial lateral line pressure measurements. Assume the total number of fishbots N is known. The particle filter running onboard the kth fishbot is described. The particle filter approximates a recursive Bayesian estimator by using a collection of P particles $\{\boldsymbol{X}_{s|s}^{(p)}\}_{p=1}^{P}$ to represent the posterior probability density function $p(\boldsymbol{X})$ at time t_s. Each particle $\boldsymbol{X}_{s|s}^{(p)} \in \mathcal{X}^{N-1}$ is a hypothesis of the $N-1$ fishbot states and higher particle densities indicate higher probability. The filter is summarized in Algorithm 1 and detailed in the following.

A. Particle Initialization

When initializing a particle $\boldsymbol{X}_{0|0}^{(p)}$ (at time t_0) the relative position of all $N-1$ neighbors is drawn randomly from the uniform distribution over the disk

$$D = \{(a_{kj}, b_{kj}) \in \mathbb{R}^2 \mid \sqrt{a_{kj}^2 + b_{kj}^2} \leq R_{\max}\}\ , \tag{16}$$

where $R_{\max}$ is the maximum relative range for estimation and the heading θ_{kj} is drawn from the uniform distribution over $\mathbb{S}$. This initialization process is repeated for all P particles. Once a measurement $\boldsymbol{y}_1$ is obtained, the particle filter (Alg. 1) processes the initialized particles $\{\boldsymbol{X}_{0|0}^{(p)}\}_{p=1}^{P}$ to give a posterior particle set $\{\boldsymbol{X}_{1|1}^{(p)}\}_{p=1}^{P}$.

Algorithm 1 Particle filter onboard the kth fishbot

1: **Input:** Measurement $\boldsymbol{y}_s$ and input u_{s-1}
2: **Input:** Prior particle set $\{\boldsymbol{X}_{s-1|s-1}^{(p)}\}_{p=1}^{P}$
3: **for** $p = 1, \ldots, P$ **do**
4: Sample process noise: $\boldsymbol{w}^{(p)} \sim \mathcal{N}(\boldsymbol{0}, \boldsymbol{\Sigma}_w)$
5: Motion update: $\boldsymbol{X}_{s|s-1}^{(p)} = \boldsymbol{F}(\boldsymbol{X}_{s-1|s-1}^{(p)}, u_{s-1}) + \boldsymbol{w}^{(p)}$
6: Calculate weight: $\tilde{w}^{(p)} = \mathcal{L}(\boldsymbol{X}_{s|s-1}^{(p)} \mid \boldsymbol{y}_s)$
7: **end for**
8: Normalize: $w^{(p)} = \tilde{w}^{(p)} / \sum_{j=1}^{P} \tilde{w}^{(j)}$, $\forall\ p = 1, \ldots, P$
9: **for** $p = 1, \ldots, P$ **do**
10: Select an index $j \in \{1, \ldots, P\}$ with probability $w^{(j)}$
11: Resample: $\boldsymbol{X}_{s|s}^{(p)} \leftarrow \boldsymbol{X}_{s|s-1}^{(j)}$
12: Sample roughening noise: $\Delta\boldsymbol{X}^{(p)} \sim \mathcal{N}(\boldsymbol{0}, \boldsymbol{D})$
13: Roughen: $\boldsymbol{X}_{s|s}^{(p)} \leftarrow \boldsymbol{X}_{s|s}^{(p)} + \Delta\boldsymbol{X}^{(p)}$
14: **end for**
15: **Output:** Posterior particle set: $\{\boldsymbol{X}_{s|s}^{(p)}\}_{p=1}^{P}$

B. Motion Update

The posterior set of particles $\{\boldsymbol{X}_{s-1|s-1}^{(p)}\}_{p=1}^{P}$ from time t_{s-1} is propagated through the discrete-time dynamics

$$\boldsymbol{X}_{s|s-1}^{(p)} = \boldsymbol{F}(\boldsymbol{X}_{s-1|s-1}^{(p)}, u_{s-1}) + \boldsymbol{w}^{(p)} \tag{17}$$

for $p = 1, \ldots, P$, to give the motion-updated particles $\{\boldsymbol{X}_{s|s-1}^{(p)}\}_{p=1}^{P}$ at time t_s (Alg. 1, lines 4–5). In (17), $\boldsymbol{F}(\cdot, \cdot)$ is a mapping that applies (9)–(10) $N-1$ times to each triplet $(a_{kj}, b_{kj}, \theta_{kj})$ contained in the particle $\boldsymbol{X}_{s-1|s-1}^{(p)}$, u_{s-1} is the kth fishbot's constant control applied for time $t \in [t_{s-1}, t_s]$, and $\boldsymbol{w}^{(p)} \sim \mathcal{N}(\boldsymbol{0}, \boldsymbol{\Sigma}_w)$ is a random zero-mean vector with covariance $\boldsymbol{\Sigma}_w = \mathrm{diag}([\sigma_{ab}^2\ \sigma_{ab}^2\ \sigma_{\theta}^2]^{\mathrm{T}})$, where σ_{ab}^2 and σ_{θ}^2 are relative position and heading variances, respectively. The process noise $\boldsymbol{w}^{(p)}$ helps to account for the idealized assumption in (9)–(10) that all neighboring fishbots have zero turn rate, when in fact they may be turning.

C. Likelihood Function

The particle filter runs at regular intervals each time a new measurement $\boldsymbol{y}_s$ is received according to (15). After the motion update, each particle $\boldsymbol{X}_{s|s-1}^{(p)}$ is assigned a weight based on the relative likelihood of the state $\boldsymbol{X}_{s|s-1}^{(p)}$ given the measurement $\boldsymbol{y}_s$ (Alg.1, line 6) using the likelihood function

$$\mathcal{L}(\boldsymbol{X}_{s|s-1}^{(p)} \mid \boldsymbol{y}_s) = I_D(\boldsymbol{X}_{s|s-1}^{(p)}) g(\boldsymbol{y}_s; \boldsymbol{h}(\boldsymbol{X}_{s|s-1}^{(p)}), \boldsymbol{\Sigma}_y)\ , \tag{18}$$

where $I_D : \mathcal{X}^{N-1} \to \{0, 1\}$ is an indicator function that maps a particle $\boldsymbol{X}_{s|s-1}^{(p)}$ to 1 if $\boldsymbol{X}_{s|s-1}^{(p)} \in \mathcal{X}_D^{N-1}$ and to zero otherwise (where $\mathcal{X}_D$ denotes the subset of $\mathcal{X}$ for which the relative position pairs (a_{kj}, b_{kj}) lie inside the disk (16)),

$$g(\boldsymbol{z}; \boldsymbol{\mu}, \boldsymbol{\Sigma}) = \frac{\exp(-\frac{1}{2}(\boldsymbol{z} - \boldsymbol{\mu})^{\mathrm{T}} \boldsymbol{\Sigma}^{-1} (\boldsymbol{z} - \boldsymbol{\mu}))}{\sqrt{(2\pi)^{N_z} |\boldsymbol{\Sigma}|}}$$

is a multivariate Gaussian probability density function for a random vector $\boldsymbol{z}$ with mean $\boldsymbol{\mu}$ and covariance $\boldsymbol{\Sigma}$, and $\boldsymbol{h}(\boldsymbol{X}_{s|s-1}^{(p)})$ is the output in (15). The indicator function prevents the filter from keeping particles that are a relative distance $\boldsymbol{R}_{\max}$ away from the estimating fishbot; above a certain distance the magnitude of the pressure signal induced by other fishbots is smaller than the sensor noise. Smaller choices of $\boldsymbol{R}_{\max}$ can benefit the filter by more densely populating the state space.

D. Particle Resampling and Roughening

After the likelihood weights are computed with (18) the particles are normalized, resampled, and roughened (Alg. 1, lines 8–14). The particle set is resampled by selecting the motion-updated particles with probability in proportion to their likelihood weights [17, p. 467]. This strategy samples particles in state-space regions with high likelihood more frequently; however, it also leads to duplicate particles (especially if a few particles have the majority of the likelihood). Duplicate particles take on distinct values during the next iteration of the motion update due to the addition of random process noise and a roughening approach that helps avoid sample impoverishment. Roughening perturbs each particle by $\Delta\boldsymbol{X}^{(p)}$ (Alg. 1, lines 12–13) sampled from a Gaussian zero-mean distribution with a $3(N-1)\times 3(N-1)$ covariance matrix $\boldsymbol{D} = \beta \mathrm{diag}(\boldsymbol{m}_k)$, where β is a fixed roughening-gain parameter and $\boldsymbol{m}_k$ is an adaptively determined vector that characterizes the spread of the current particle population as described in [18]. The sensor noise covariance matrix $\boldsymbol{\Sigma}_y$ in (18) is also used to tune filter performance. A likelihood function with a narrow peak in $\mathcal{X}_D^{N-1}$ can make it challenging to identify high-likelihood particles. Artificially inflating $\boldsymbol{\Sigma}_y$ widens the peak and can improve reliability. Once the particles are resampled and roughened the posterior set $\{\boldsymbol{X}_{s|s}^{(p)}\}_{p=1}^{P}$ becomes the prior for the next iteration.

E. Example

The particle filter's output is illustrated in Fig. 2 for $N = 2$ fishbots. The initialized set of particles with a uniform distribution over $\mathcal{X}_D$ is shown in Fig. 2a. After 25 measurements the relative position estimate is close to the true value but there remains a bias in relative heading histogram. After 100 measurements both the position and relative heading converge tightly around the true values.

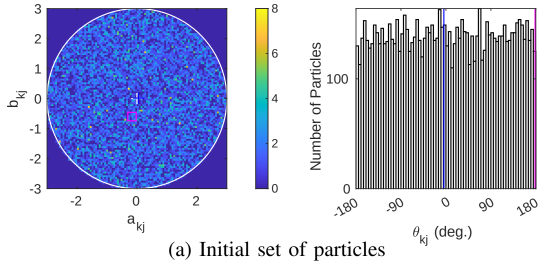

(a) Initial set of particles

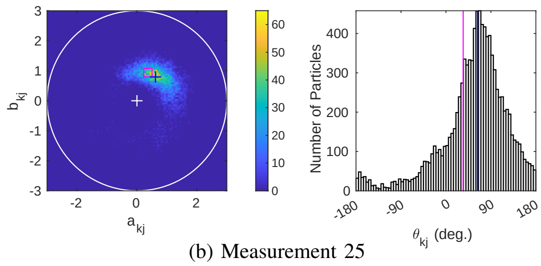

(b) Measurement 25

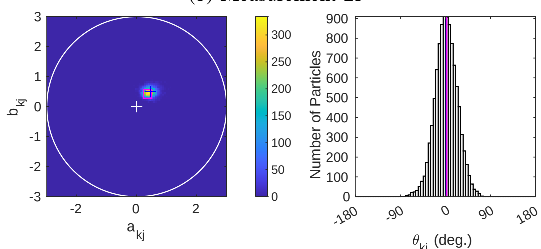

(c) Measurement 100

Fig. 2: Snapshots of particle filter state at three measurement times for simulation with $N = 2$ fishbots (see Fig. 3a). Left: histogram of particles in the a_{kj}–b_{kj} plane with white the circle indicating $R_{\max}$ boundary, magenta square indicating the true relative position, and blue crosshairs indicating the estimated relative position. Right: histogram of particles with magenta line indicating the true relative heading and the blue line indicating the estimated relative heading.

V. Parallel Formation Control

For the fishbots to synchronize their heading and achieve a parallel formation, each fishbot runs an independent particle filter of the form described in Sec. IV and extracts from the posterior particle set an estimate of the relative heading $\hat{\theta}_{kj}$ of the $N-1$ other fishbots. The estimated relative heading is used with the output-feedback control law

$$u_k = \frac{K}{N} \sum_{j=1}^{N} \sin \hat{\theta}_{kj} \; . \tag{19}$$

If the estimates converge to their true values, $\hat{\theta}_{kj} \to \theta_{kj}$, then (19) converges to (3) and the estimation onboard each fishbot is equivalent to the exchange of heading information in an undirected all-to-all communication topology.

To estimate $\hat{\theta}_{kj}$ for each fishbot, the relative heading angles across all particles are collected in a set $\mathbf{\Theta}$. Since $\mathbf{\Theta}$ contains circular data it is decomposed into planar components $\boldsymbol{T} = \{(\cos\theta_{kj}^{(q)}, \sin\theta_{kj}^{(q)})\}$ for all $q = 1, \ldots, (N-1)P$. A 2D Gaussian mixture model (GMM) with $N-1$ components is constructed to model the the two-dimensional data in $\boldsymbol{T}$. Let $(\mu_{j,1}, \mu_{j,2})$ correspond to the mean of the jth Gaussian mixture component. The estimated heading is then

$$\hat{\theta}_{kj} = \mathrm{atan}(\mu_{j,2}/\mu_{j,1}) \; . \tag{20}$$

A similar approach using a GMM estimates $\hat{a}_{kj}, \hat{b}_{kj}$. These values can be used for circular and other formations [16]. The observer-based parallel formation control (19)–(20) is demonstrated through simulations as described next.

A. Simulation Setup

Numerical simulations of the output feedback formation controller use the parameters from Table I and assume pressure sensors are distributed symmetrically around the perimeter of each fishbot's body (represented by a hydrofoil shape) as shown in Fig. 1. Each simulation numerically integrates the continuous dynamics (8) and, periodically at fixed sampling intervals T, runs the filter Alg. 1 and evaluates the control (19) with (20) independently for each fishbot (refer to the video attachment accompanying this paper). Interaction between the fishbots is purely hydrodynamic and utilizes no other means of communicating state information.

TABLE I: Parameters used in numerical simulations. Dashed lines separate parameters related to the fishbot dynamics and the dipole flow and measurement models; the estimation strategy; and the parallel formation control law.

Parameter	Symbol	Value
Sensing/control period	T	0.1 s
Dipole length	l	0.2 m
Nominal velocity	v	0.2 m/s
Number of pressure sensors	N_s	5
Water density	ρ	1000 kg/m^3
Process noise, position	σ_{ab}^2	$(0.1T)^2$ m^2
Process noise, heading	σ_θ^2	$(5T)^2$ deg^2
Max. range hypothesis	$R_{\max}$	3 m
Filter roughening gain	β	0.001
Parallel formation control gain	K	1

B. Simulation Results with $N = 2$ Robots

For $N = 2$ fishbots, the particle filter uses $P = 10,000$ particles and actual measurement noise variance $\sigma_y^2 = 10$ Pa^2. Two representative scenarios are shown with the fishbots in an inward-facing (Fig. 3a) and outward-facing (Fig. 3b) initial configurations. In each case, the pair of fishbots achieves a parallel formation within 150 measurements. The pressure fluctuations are greatest during maneuvers where the fishbots are in close proximity and then settle to constant values once the formation is achieved. The filter works well for a wide range of initial conditions and parameter values.

C. Simulation Result with $N = 3$ Robots

For $N = 3$ fishbots, the size of the state-space necessitated more particles ($P = 20,000$) to be used with the filter. Also, a smaller likelihood variance $\sigma_y^2 = 0.5$ Pa^2 is selected. When simulating $N = 3$ fishbots in Fig. 3c, an informed prior is used to initialize the particles by drawing the relative-position of the particles from a multi-variate Gaussian distribution around the correct mean position with variance of one dipole length. The relative headings of the particles are initially random. The informed prior is used so that the framework may be demonstrated with a computational tractable number of particles. In principle, a larger number of particles with an un-informed prior should produce similar results. This modification highlights the computational challenges associated

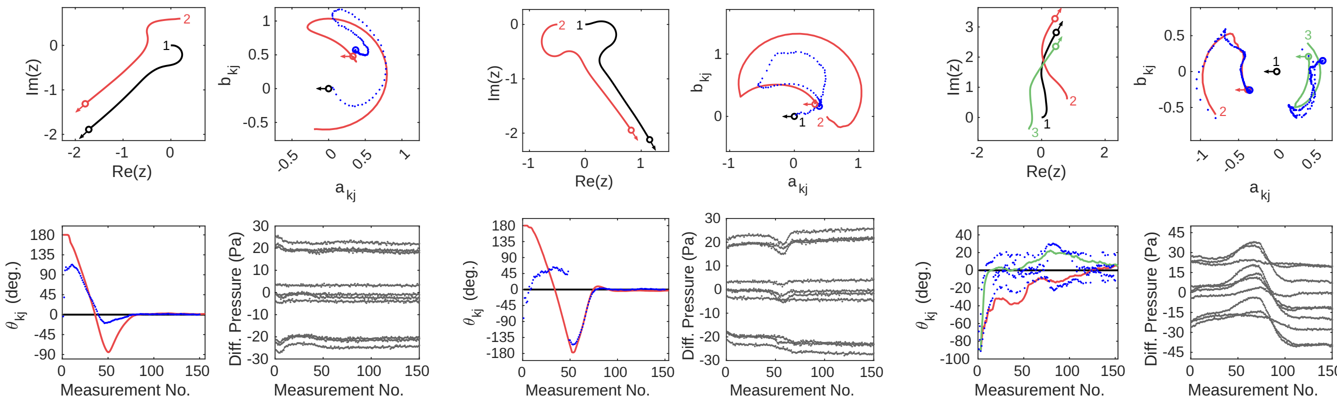

(a) $N = 2$, initially inward-facing (b) $N = 2$, initially outward-facing (c) $N = 3$

Fig. 3: Simulation results for three scenarios. Top left of each subfigure: track of fishbots in $\mathcal{I}$ frame with starting location adjacent to agent number with the final orientation of fishbots indicated by an arrow. Top right: Track of fishbots as viewed in frame $\mathcal{B}_k$ from perspective of first agent ($k = 1$) with the final orientation of fishbots indicated by an arrow. Blue dots are estimates of the relative position and the blue circle indicates the estimates at the end of the simulation. Bottom left: True relative heading of fishbots with respect to agent 1 and blue dots are estimates of the relative heading. Bottom right: differential pressure sensor measurements.

with estimating multiple fishbots on a single computer; the performance of the filter with $N = 3$ fishbots is sensitive to the choice of initial conditions/parameters. Although the heading estimate is noisy compared to the $N = 2$ cases, the fishbots align to within 5 deg. after 150 measurements.

VI. Conclusion

This paper described an output feedback control framework that uses pressure feedback from a noisy artificial lateral line sensor to achieve parallel formations for a school of robotic fish. The fishbots are modeled as self-propelled particles that produce a dipole potential flow. This flow model serves as the basis for the likelihood function in a particle filter to infer the relative positions and heading of other fishbots. The particle filter is formulated in the path frame and runs independently onboard each fishbot. Numerical simulations demonstrate that the proposed output feedback framework achieves parallel formations with $N = 2$ and $N = 3$ fishbots for a range of initial conditions. The approach is limited to close-proximity fishrobot configurations that allow detection of hydrodynamic cues in the presence of sensor noise. Practical implementation of the particle filter estimation approach would require substantial onboard computational resources. Future work should consider alternative filtering techniques that improve computational efficiency, robustness for a larger number of fishbots, allow estimating an unknown number of fishbots, and utilize more realistic flow models that incorporate vortex shedding. The output feedback control framework can also be modified to achieve circular and other planar formations.

References

[1] B. L. Partridge and T. J. Pitcher, "The sensory basis of fish schools: Relative roles of lateral line and vision," *J. Comparative Physiology*, vol. 135, no. 4, pp. 315–325, 1980.

[2] L. DeVries, F. D. Lagor, H. Lei, X. Tan, and D. A. Paley, "Distributed flow estimation and closed-loop control of an underwater vehicle with a multi-modal artificial lateral line," *Bioinsp. & Biomim.*, vol. 10, no. 2, p. 025002, 2015.

[3] F. Zhang, F. D. Lagor, D. Yeo, P. Washington, and D. A. Paley, "Distributed flow sensing for closed-loop speed control of a flexible fish robot," *Bioinsp. & Biomim.*, vol. 10, no. 6, p. 065001, 2015.

[4] J. Zheng, X. Zheng, T. Zhang, M. Xiong, and G. Xie, "Dual-sensor fusion based attitude holding of a fin-actuated robotic fish," *Bioinsp. & Biomim.*, vol. 15, no. 4, p. 046003, 2020.

[5] W. K. Yen, D. M. Sierra, and J. Guo, "Controlling a robotic fish to swim along a wall using hydrodynamic pressure feedback," *IEEE J. Oceanic Engineering*, vol. 43, no. 2, pp. 369–380, 2018.

[6] K. Nelson and K. Mohseni, "Hydrodynamic force decoupling using a distributed sensory system," *IEEE Robotics and Automation Letters*, vol. 5, no. 2, pp. 3235–3242, 2020.

[7] F. Zhang, P. Washington, and D. A. Paley, "A flexible, reaction-wheel-driven fish robot: Flow sensing and flow-relative control," in *American Control Conf.*, 2016, pp. 1221–1226.

[8] B. A. Free and D. A. Paley, "Model-based observer and feedback control design for a rigid Joukowski foil in a Kármán vortex street," *Bioinsp. & Biomim.*, vol. 13, no. 3, p. 035001, 2018.

[9] W. K. Yen, C. F. Huang, H. R. Chang, and J. Guo, "Localization of a leading robotic fish using a pressure sensor array on its following vehicle," *Bioinsp. & Biomim.*, vol. 16, no. 1, p. 016007, 2021.

[10] X. Zheng, W. Wang, L. Li, and G. Xie, "Artificial lateral line based relative state estimation between an upstream oscillating fin and a downstream robotic fish," *Bioinsp. & Biomim.*, vol. 16, no. 1, p. 016002, 2021.

[11] P. Weber, G. Arampatzis, G. Novati, S. Verma, C. Papadimitriou, and P. Koumoutsakos, "Optimal flow sensing for schooling swimmers," *Biomimetics*, vol. 5, no. 1, pp. 1–22, 2020.

[12] T. Salumäe and M. Kruusmaa, "Flow-relative control of an underwater robot," *Proc. Royal Society A: Math., Phys. Eng. Sci.*, vol. 469, no. 2153, p. 20120671, 2013.

[13] E. Kanso and A. C. H. Tsang, "Dipole models of self-propelled bodies," *Fluid Dynamics Research*, vol. 46, no. 6, p. 061407, 2014.

[14] A. T. Abdulsadda and X. Tan, "Nonlinear estimation-based dipole source localization for artificial lateral line systems," *Bioinsp. & Biomim.*, vol. 8, no. 2, p. 026005, 2013.

[15] E. W. Justh and P. Krishnaprasad, "Equilibria and steering laws for planar formations," *System & Control Letters*, vol. 52, no. 1, pp. 25–38, 2004.

[16] R. Sepulchre, D. A. Paley, and N. E. Leonard, "Stabilization of planar collective motion: All-to-all communication," *IEEE Trans. Automatic Control*, vol. 52, no. 5, pp. 811–824, 2007.

[17] D. Simon, *Optimal State Estimation: Kalman, H_∞ and Nonlinear Approaches*. Wiley, 2006.

[18] N. J. Gordon, D. J. Salmond, and A. F. Smith, "Novel approach to nonlinear/non-Gaussian Bayesian state estimation," in *IEE Proc. F - Radar and Signal Processing*, vol. 140, no. 2, 1993, pp. 107–113.